Calcination Kinetics and Surface Area of Dispersed Limestone Particles

The rates of calcination of two types of limestones, ranging in particle size from 1 to 90 μm, were measured over the temperature range 516 to 1,000°C. A kinetic model based on the B.E.T. (Brunauer-Emmett-Teller method) surface area of the $CaCO_3$ correlates the results over 5 orders of magnitude in reaction rate. The B.E.T. surface area of CaO formed by rapid calcination in dispersed-particle systems is 50 to 90 m^2/g.

R. H. BORGWARDT

Special Projects Office
Industrial Environmental Research Laboratory
U.S. Environmental Protection Agency
Research Triangle Park, NC 27711

SCOPE

Acid rain is recognized as a problem of increasing importance to the industrialized areas of the world that derive a major part of their energy requirements from coal combustion. A principal cause of acid rain is generally attributed to the sulfur oxides (SO_x) and the nitrogen oxides (NO_x) emitted by electric power plants. Effective pollution control technologies have been developed for these emissions and are now being installed on new plants. The most widely accepted technologies are combustion modification (for NO_x) and wet or dry scrubbing (for SO_x). The application of these two independent controls is a costly solution to the problem. A chemical engineering challenge for the 1980s is to design a single control system for both NO_x and SO_x that is less expensive and is retrofitable to existing plants. The Environmental Protection Agency has initiated a program to evaluate the limestone-injection multistage burner (LIMB) to fill this need. This approach involves the injection of pulverized limestone into a staged burner designed for NO_x reduction; the limestone can capture sulfur by gas/solid reactions with H_2S and COS in the reducing zone of the burner and by reaction with SO_2 in the oxidizing zone. In the reducing zone, reactions with either $CaCO_3$ or CaO are possible; the dominant mechanism is determined in part by calcination kinetics. The effective residence time for reactions involving CaO will also depend on the rate of decomposition of the $CaCO_3$.

This study concerns the calcination rate of small limestone particles appropriate to the LIMB process. Although the decomposition of pure $CaCO_3$ has been previously studied by many investigators, there is still no consensus on the mechanism. Mass transfer, heat transfer, chemical kinetics, and combinations of these have all been reported as rate-limiting. As a result, the prior work does not provide a clear basis for predicting the calcination rate of small particles in a high-temperature dispersed system such as LIMB. There is substantial evidence that the calcination kinetics also affect the reactivity of the CaO product by influencing its grain size and specific surface area. The limited data available on calcination in a dispersed system suggest that the surface areas are extraordinarily large immediately following the decomposition of $CaCO_3$. Because those data were obtained from particles collected in a flue gas atmosphere, they were unable to establish an accurate value, or range of values, for the CaO surface area. In addition to establishing the rate of calcination and the rate limiting mechanism for small particles in a dispersed system, the objective of this study is also to obtain accurate B.E.T. measurements of the CaO surface area produced under such conditions.

Rate measurements were made in two types of isothermal systems: a differential reactor at temperatures from 475 to 710°C, and an entrained flow reactor at temperatures from 775 to 1,000°C. Nitrogen sweep gas was used to ensure that neither the rate measurements nor the B.E.T. measurements were influenced by the reverse carbonation reaction. Differential conditions were ensured by use of small sample size, high gas velocity, and low particle dispersion density. The particle size was varied from 1 to 90 μm in the differential reactor and from 10 to 90 μm in the flow reactor, using two naturally occurring limestones representing markedly different physical and geological properties.

CONCLUSIONS AND SIGNIFICANCE

When the resistances of intraparticle and interparticle mass transfer are eliminated, the calcination rate of small limestone particles can be described by a model that assumes a direct relationship with the B.E.T. surface area of the $CaCO_3$. Difficulties of prior studies with small particles are resolved by providing adequate particle dispersion and high throughput of inert sweep gas. Under these conditions, the measured rate constant is 2.5×10^{-8} $mol/cm^2 \cdot s$ at 670°C with an estimated error of ±1.0, based on 16 determinations with two different types of limestones ranging in particle size from 1 to 90 μm. The model satisfactorily predicts the rate of calcination in a dispersed system at temperatures up to 1,000°C and 80% conversion of 10 μm particles. The apparent activation energy for calcination of limestone particles in a dispersed system is consistent with the value reported for the chemically controlled decomposition reaction, and this agreement is maintained over 5 orders of magnitude in reaction rate. On the basis of these measurements and those of other investigators, the apparent activation energy is estimated to be 49 ± 2 kcal/mol (205 ± 8 kJ/mol). The B.E.T. surface area of CaO generated when small particles are calcined under chemical reaction control is 50 to 60 m^2/g—an order of magnitude greater than that of commercial lime. Since current grain theories predict a strong relationship between B.E.T. surface area and CaO reactivity, calcination kinetics can be expected to have a significant effect on the performance of dispersed gas/solid systems based on limestone. Such systems will include the limestone-injection multistage burners being developed to control the emission of acid rain precursors from coal-fired power plants.

INTRODUCTION

As pointed out by Satterfield and Feakes (1959), the thermal decomposition of $CaCO_3$ involves three potential rate controlling processes: (1) heat transfer to the surface and then through the CaO product layer to the reaction interface, (2) mass transfer of CO_2 away from the interface through the product layer, and (3) the chemical reaction. From their study of 2-cm-dia. cylinders, calcined in CO_2 atmosphere, they concluded that heat transfer is the major rate controlling factor. Because temperatures measured in the $CaCO_3$ core were consistently greater than the equilibrium decomposition temperature, they also concluded that chemical reaction is an important factor. Hills (1968) took issue with these conclusions, especially with regard to chemical reaction. In a comprehensive study of 1-cm-dia. spheres, calcined in air and air/CO_2 mixtures, he found the process controlled exclusively by heat transfer to the solid surface and by mass transfer of CO_2 through the product layer. Although Satterfield and Feakes found no significant mass transfer resistance, the latter point is not a contradication because severe sintering occurred at the higher temperatures and longer calcination periods used for their study; sintering enlarges the CaO pores and cracks the product layer (by shrinkage), both of which enhance CO_2 diffusion.

Even though the product layer is apparently a major resistance to mass transfer in large spheres calcined under mild conditions, its effect should diminish as the size of the $CaCO_3$ is reduced. Since the product layer becomes vanishingly thin in micrometer-size particles, the effect of chemical reaction, if any, should be more prominent. Nevertheless, most studies of the calcination rate of small particles have failed to reveal any resistance other than heat transfer: Gallagher and Johnson (1976) studied the rate of decomposition of 30 μm $CaCO_3$ in a thermal gravimetric analyzer (TGA) at 900 to 950°C, in a CO_2 atmosphere, and concluded that the rate was determined by thermal transport. Caldwell et al. (1977), also using TGA techniques, reached the same conclusion when comparing the calcination rates of 30 μm $CaCO_3$ particles in three different sweep gases: He, Ar, and N_2. They found the rates to increase with the thermal conductivity of the gas atmosphere at temperatures of 550 to 680°C.

A study of the calcination rate of 90 μm limestone particles entrained in flue gas at high temperatures (870 to 1,100°C) was carried out for the Environmental Protection Agency by Battelle Memorial Institute (Coutant et al., 1970, 1971). That study, done in a dispersed-particle flow reactor with short residence times (0.1 to 2 s), most closely simulates the reaction conditions in the limestone-injection multistage burner (LIMB). Their data were analyzed with a theoretical model based on the assumption that the overall rate is controlled exclusively by heat and mass transfer. The observed calcination rates were about half those predicted by the model and, for the only test made with 50 μm particles, the rate was one-tenth as fast as the model's prediction. In this case, a slower process seems to control.

The argument supporting chemical reaction as an important resistance to $CaCO_3$ calcination was revived by Beruto and Searcy (1974), who reviewed the results of ten published studies of the reaction and concluded that most of those measurements, which used powdered samples and TGA techniques, were dominated by the effects of interparticle diffusion (i.e., the rate measurements were made at conditions that were not differential with respect to CO_2). They argue that these effects are responsible for the fact that the reported activation energies were generally near that of the equilibrium decomposition, 39.1 to 40.5 kcal/mol (163.8 to 169.7 kJ/mol). They demonstrated that vacuum calcination, which eliminates diffusion resistances, yields an apparent activation energy of 49 kcal/mol (205 kJ/mol) which is well above the values expected for equilibrium decomposition. The conclusion is supported by a datum of Gallagher and Johnson (1973) who measured an apparent activation energy of 49.7 kcal/mol (208 kJ/mol) in a TGA when the $CaCO_3$ sample was reduced to the minimum size of 1 mg.

Further studies of vacuum calcination were made by Powell and Searcy (1980) with thin single crystals of calcite, which yielded a value of 50 kcal/mol (209.5 kJ/mol) for the activation energy over the temperature range 636 to 844°C. On the basis of their measurements and three others reported in the literature at experimental conditions that minimize the diffusion resistances, they placed a value of 49 ± 3 kcal/mol (205 ± 12.6 kJ/mol) on the true activation energy of the reaction. The reaction rate, based on the dimensions of the flat crystal face, was evaluated at 1.0×10^{-6} mol/cm^2-s at 844°C. If, in the absence of diffusional resistance, the rate of $CaCO_3$ decomposition is indeed dominated by chemical resistance, then these kinetic parameters should be reconcilable with the observed calcination rates of small particles in the dispersed system represented by Coutant's data. The objective of this study is to make that comparison over as broad a range of temperature and particle size as possible.

Another objective of this study is to determine the B.E.T. (Brunauer-Emmett-Teller method) surface area of CaO formed by high temperature "flash" calcination of limestone particles in a dispersed system. Current grain theories predict that the B.E.T. surface area of a solid should be strongly related to its reactivity with a gas. The reaction rate of SO_2 with CaO has been directly related to its specific surface area (Borgwardt and Harvey, 1972). Large particles of limestone calcined in a rotary kiln at 980°C normally yield surface areas of only 2 to 5 m^2/g. Glasson (1958) found that a surface area of 43 m^2/g can be attained by vacuum calcination at 750°C and showed that the specific surface area decreases with increasing temperature and time due to sintering; i.e., growth of the CaO grains. Beruto et al. (1980) reported a B.E.T. surface area of 78 m^2/g for vacuum calcination at 513°C. Chan et al. (1970) attained a surface area of 24.6 m^2/g calcining limestone particles in a TGA at 745°C. Like other TGA studies, the flow rate of nitrogen sweep gas was necessarily low and the calcination was non-differential, as indicated by the reported variation of decomposition rate with sample size.

The limited data available on calcination in a dispersed system suggest that very large B.E.T. surface areas may exist immediately after the rapid decomposition of $CaCO_3$, even at high temperatures. Coutant et al. (1971) measured several values as large as 60 m^2/g when 90 μm limestone particles were calcined in less than 1 s at 1,100°C. Due to the flue gas atmosphere, however, the B.E.T. measurements were highly variable and uncertain; recarbonation and hydration of the CaO were possible during sample collection. Those results nevertheless suggest that the surface area of CaO is related to the calcination rate and that the relationship must be understood if sulfur capture in LIMB is to be predicted from process variables and chemical kinetics.

EXPERIMENTAL

Approach

The experimental problems associated with TGA measurements of the $CaCO_3$ decomposition kinetics of small particles have been discussed by Gallagher and Johnson (1973). Those problems are resolved in this study by use of a differential reactor which can operate with higher throughput of sweep gas (by a factor of 400) and smaller particle dispersion densities—defined as the mass of particles per cross-sectional area of the sample holder. Additional measurements were made in an entrained-particle flow reactor which permitted the temperature range to be extended beyond that of any prior study. By comparison of the rates obtained in these two different types of gas/solid contactors, any discontinuities that would signal a change in the rate limiting mechanism should be readily apparent.

The general term "differential reactor," as applied to gas/solid reactions, means that the difference in reactant gas concentration between the reactor feed and effluent is not significantly affected by the reaction under study. This condition must be met in any case for valid kinetic data. In the case of limestone calcination, which is a reversible reaction, "differential conditions" require that the CO_2 evolved from a given particle does not interfere with the rate of decomposition of neighboring particles. Ingraham and Marier (1963) showed that the rate of decomposition is proportional to the difference between the equilibrium partial pressure of CO_2 at the given temperature and the ambient CO_2 partial pressure surrounding the particles. To achieve differential conditions under these circumstances thus

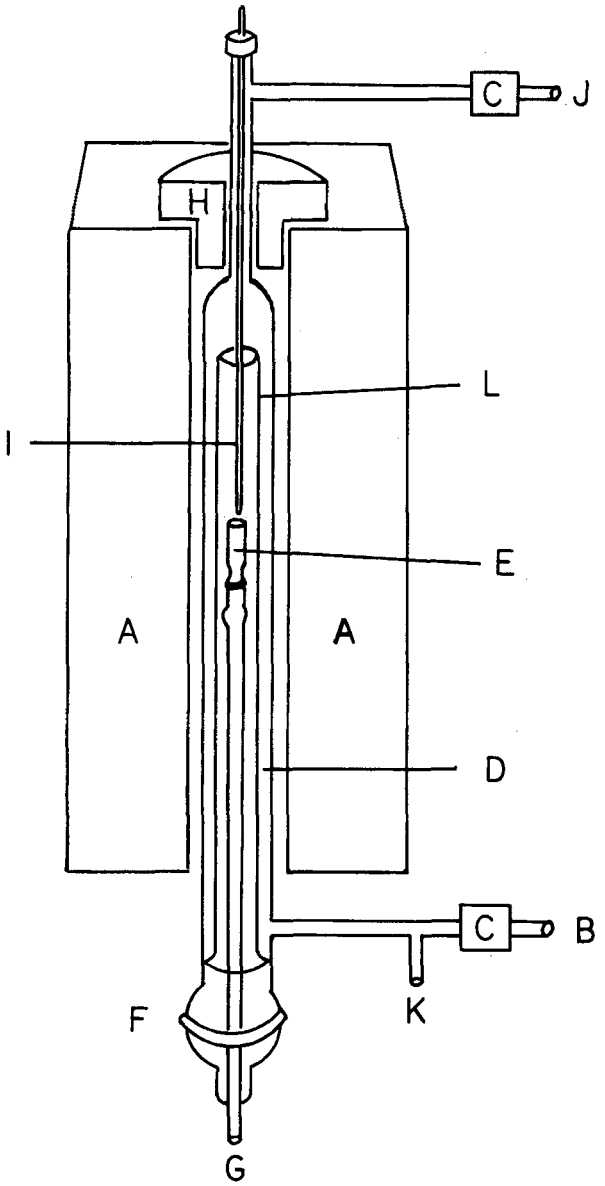

Figure 1. Differential reactor: (A) electric furnace, (B) gas inlet, (C) solenoid valve, (D) gas preheat zone, (E) limestone sample holder, (F) ball joint, (G) gas exhaust, (H) ceramic plug, (I) thermocouple, (J) CO_2 gas inlet, (K) manometer connection, and (L) reactor tube.

requires that: (1) all traces of CO_2 are removed from the sweep gas when working at low temperatures, (2) a high throughput of inert sweep gas is used to dilute and remove the CO_2 generated by the reaction, (3) the sample size is minimized to limit the local concentration of CO_2 generated, and (4) the particles are dispersed to a low density over the cross-sectional area of the reactor. It follows that differential conditions will be more difficult to attain as the specific decomposition rate of the $CaCO_3$ increases; i.e., with high temperatures and small particles. The reactor used for these studies permitted the gas flow rate and sample size to be varied over broad ranges to ensure that differential conditions were achieved at all operating conditions.

Apparatus

The differential reactor was fabricated of quartz glass as shown in Figure 1. Sweep gas, obtained from a liquid nitrogen tank and purified with an Ascarite (Arthur H. Thomas Co.) filter, entered the bottom of the reactor and passed upward through a 3.0 cm I.D. × 95 cm outer shell and downward through an annular 2.0 cm I.D. × 77 cm reactor tube. The limestone sample was positioned 5 cm below the center of the furnace in a 1.4 cm I.D. removable holder which was sealed to the exhaust tube by a ground glass joint as shown in Figure 2. The limestone particles were dispersed into a quartz wool substrate (Thermal American Fused Quartz Co.) through which the entire gas flow passed. The sample-holder/exhaust-tube assembly, normally containing 10 mg of limestone particles, was inserted at the bottom of the reactor through a ball joint which sealed it into the gas preheater formed by the annular space between the two larger tubes. The upper 60 cm of the reactor was heated by an electric furnace.

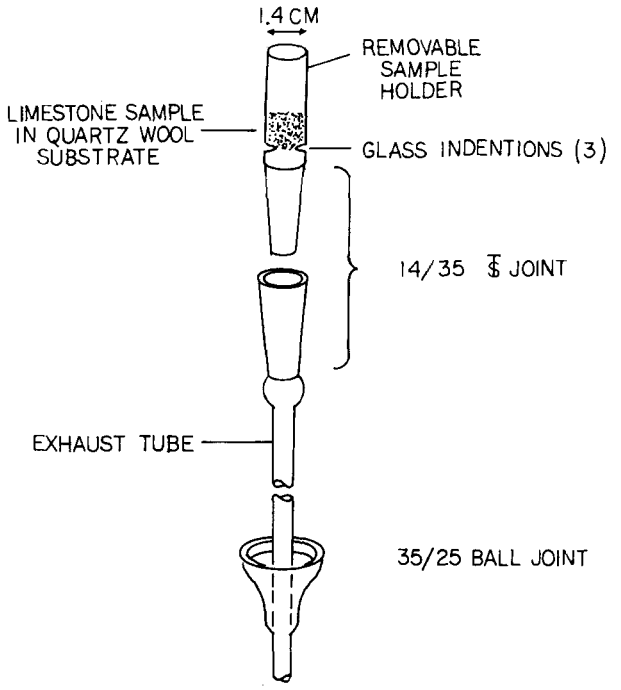

Figure 2. Differential reactor: detail of limestone sampler-holder/exhaust-tube assembly.

The reactor is operated in the following manner: The sample holder, loaded with the quartz wool, is inserted into the reactor and exposed to the operating sweep gas, withdrawn, cooled to room temperature in flowing N_2, and weighed. This treatment removes any wool fragments produced during loading (typically 0.3 mg). The limestone sample is dispersed into the quartz wool and the holder re-weighed. The sample is held in the cool bottom part of the reactor for 2 min while pure CO_2 is flushed through the reactor and sample; the sample holder is then fully inserted, the CO_2 turned off, and the assembly sealed at the ball joint. The sample is allowed to heat for 9 min under 1 atm (0.1 MPa) CO_2 to reach temperature equilibrium with the reactor. The reaction is initiated by opening a valve allowing the sweep gas (normally N_2) to enter at normal flow rates, between 24 and 44 L/min. When the desired reaction period has elapsed, the N_2 sweep is terminated and the sample assembly withdrawn. The sample holder is removed, cooled under flowing N_2 to room temperature, weighed, and the contents ejected into a beaker for calcium analysis by EDTA titration. The time required to cool the sample sufficiently to quench the reaction after removal from the reactor is estimated to be less than 4 s. From the weight loss and calcium recovery, the degree of calcination of the sample is calculated. A series of runs at different reaction periods yields the conversion vs time response.

The entrained flow reactor is illustrated in Figure 3. It consists of a vertical stainless steel (Type 310) tube of 3.17 m length, electrically heated by three furnaces. Gas preheat is provided in the annular volume between the outer (4.8 cm dia.) shell and the 1.27 cm I.D. reactor tube. Nitrogen entrainment gas enters the bottom of the reactor and passes upward through the preheat zone to the top of the reactor where limestone particles are injected by means of a feed system described by Quann et al. (1982). At 925°C, the reactor volume is 422 cm^3. The gas and entrained particles pass downward through the isothermal reactor tube and leave through a water-cooled deflector pipe leading to a cyclone. The particles are collected from the cyclone directly in glass sample vials, eliminating contact with air. The maximum temperature of the gas leaving the cyclone is 150°C.

The particle feeder is capable of injecting limestone as small as 10 μm at a rate of 100 mg/min. The gas flow through the reactor is variable from 10 to 45 L/min to control particle residence time from 0.6 to 0.1 s, respectively, at temperatures of 775 to 1,100°C. The Reynolds number at maximum flow is 1,700 at 1,000°C. Degree of calcination is determined by weight loss on ignition. TGA analyses show that hydration during sample handling (from air exposure) is kept within 1%. The specific surface area of the calcines is determined by the multipoint B.E.T. method with an AccuSorb Analyzer (Micromeritics Instrument Corp.).

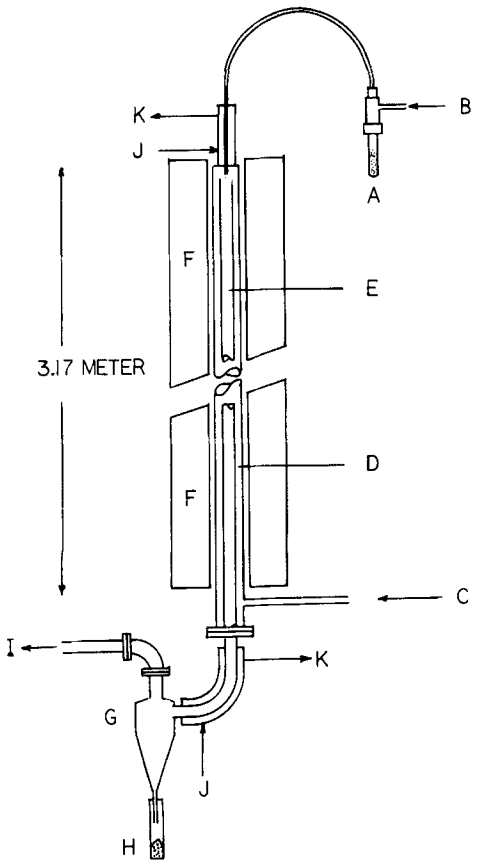

Figure 3. Entrained-flow reactor: (A) limestone feed, (B) N_2 carrier gas, (C) N_2 entrainment gas feed, (D) gas preheat zone, (E) reactor tube, (F) electric furnace, (G) cyclone, (H) CaO product, (I) gas exhaust, (J) cooling water, and (K) drain.

Materials

Two geologically dissimilar, naturally occurring limestones of 95% $CaCO_3$ purity were studied. One stone is Fredonia Valley White (BCR 2061) which is the same stone used by Coutant. It is an unconsolidated material with an average grain size of 2 μm. Mercury intrusion measurements show 8% porosity and a mean pore diameter of 0.4 μm. The other stone, Georgia Marble (BCR 1336), is a highly crystallized material with 3% porosity and mean pore diameter of 4 μm. The geological characteristics of both stones have been described by Harvey (1971). The pulverized stones (as received) were fractionated into samples of narrow particle size distribution with an Accucut Classifier (Donaldson Co., Inc.) and the mean particle diameter was determined by Coulter Counter analyses and by scanning electron microscope sizing. Since the reliability of either method is limited for particles smaller than 2 μm, measurements of B.E.T. surface areas are the principal criterion of particle size used here. They were determined by nitrogen adsorption and by krypton adsorption. Particles 50 and 90 μm diameter were obtained by sieving through 270/325 and 140/200 mesh screens.

RESULTS AND DISCUSSION

Differential Reactor

The calcination rate of 90 μm particles of stone 2061 at 720°C is shown in Figure 4. With a sweep gas velocity of 9 m/s, the calcination rate was independent of sample size up to a maximum particle dispersion density of about 40 mg/cm^2, verifying that differential conditions were attained. A test for conductive heat transfer limitation is shown in Figure 5. The N_2 sweep gas was replaced by other gases having higher thermal conductivity (He) and lower conductivity (Ar) in the manner described by Caldwell et al. (1977). The fact that calcination rate is independent of the sweep gas demonstrates that conductive heat transfer is not rate-

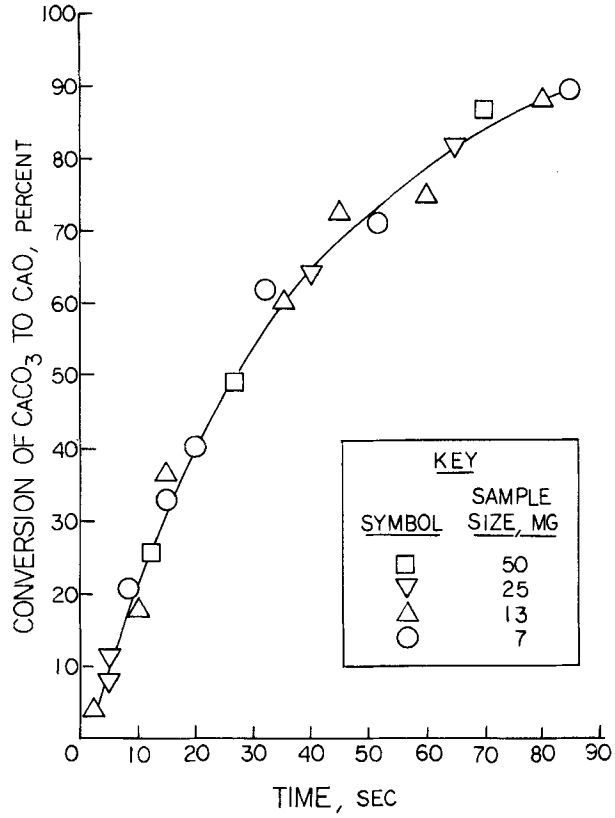

Figure 4. Calcination rate of 90 μm Fredonia limestone at 720°C; test for differential conditions: gas velocity = 9 m/s; reactor cross section = 1.5 cm^2.

controlling at the conditions used here. Two possible explanations are offered for the contrary results reported by Caldwell: (1) the sample responded thermally as a single porous mass rather than as individual particles, due to the lower gas velocity used in the TGA; or (2) the sweep gases were contaminated by trace concentrations of CO_2. Both the Ar and N_2 used in the present study were

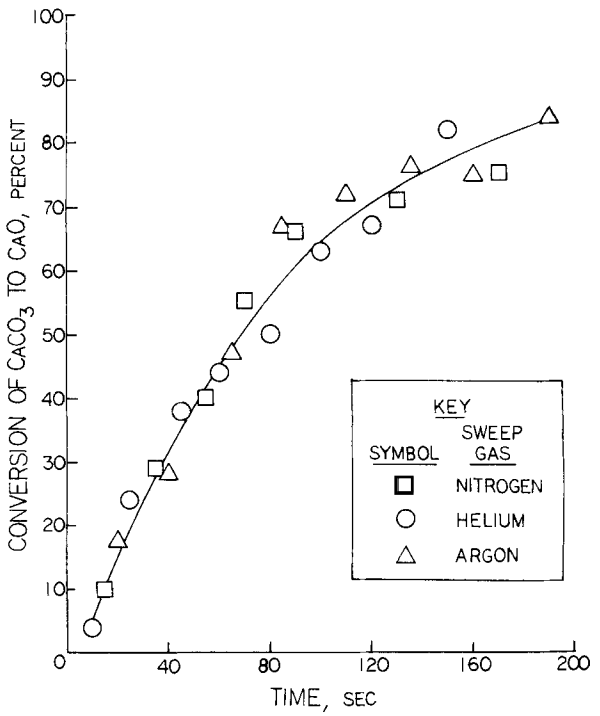

Figure 5. Test for conductive heat transfer limitation in the differential reactor, 50 μm Georgia marble at 670°C: particle dispersion = 7 mg/cm^2; gas velocity = 9 m/s.

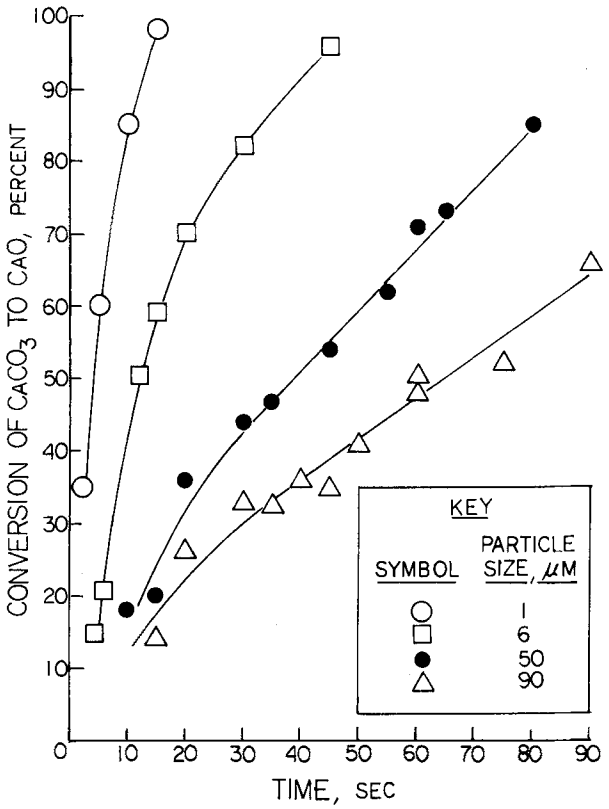

Figure 6. Calcination rate of Georgia marble as a function of particle size: temperature = 710°C; nitrogen velocity = 9 m/s; and particle dispersion = 7 mg/cm².

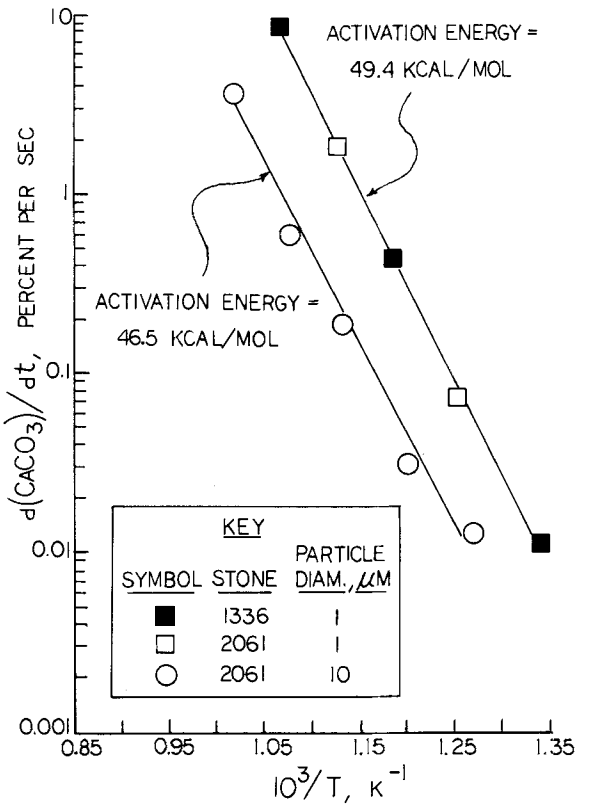

Figure 7. Calcination rate of limestone particles as a function of reactor temperature: rates evaluated at 50% conversion; gas velocity = 13 m/s.

found to contain sufficient CO_2 to affect the results, had not Ascarite been used for cleanup.

The effect of particle size on calcination rate is shown in Figure 6 for stone 1336. As particle size was reduced, higher gas velocity and smaller sample size were required to maintain differential conditions; for 1 μm particles, 13 m/s gas velocity was necessary with 10 mg samples at a maximum reactor temperature of 670°C. In Figure 7, the effect of temperature is shown as an Arrhenius plot of the reaction rates determined from the slope of the conversion vs. time responses at 50% conversion to CaO. An initial estimate of the activation energy, from the slopes of the straight lines of Figure 7, is 48 kcal/mol (201 kJ/mol).

Calcination Model

Beruto and Searcy (1974) showed that the calcination rate per unit area of a flat crystal surface is constant—the deviations noted by Hills (1968) do not occur when $CaCO_3$ decomposes without mass transfer resistance; thus,

$$\frac{d(CaCO_3)}{dt} = -k_s A_{CaCO_3} \qquad (1)$$

The diffusion of CO_2 through the product layer was shown to have no effect on the validity of Eq. 1 for CaO thicknesses to at least 800 μm at 740°C.

Limestones are not fully crystalline materials, but contain varying degrees of natural porosity. Satterfield and Feakes (1959) showed that calcination occurs in porous agglomerates as a zone-type reaction instead of the sharply defined interface that characterizes the decomposition of non-porous $CaCO_3$ crystals. The surface area contributed by the pores must therefore be taken into account when applying Eq. 1 to limestone particles. Stone 1336, with a porosity of 3%, has a B.E.T. surface area of 0.12 m²/g of 90 μm particles. Only about 20% of this area can be accounted for as external surface, assuming theoretical $CaCO_3$ particle density. Thus, about 80% of the total surface of stone 1336 is pore surface. The ratio is even larger for stone 2061 which has greater specific pore volume and surface area. As particle size is reduced, the surface of the internal pores can be expected to participate increasingly in the calcination reaction; as a limit, the A_{CaCO_3} term of Eq. 1 should be the B.E.T. surface area.

The relationship between the calcination rate of various-size limestone particles and their initial B.E.T. surface area is shown in Figure 8, as determined in the differential reactor. The rates were measured at 50% conversion and normalized to 710°C on the

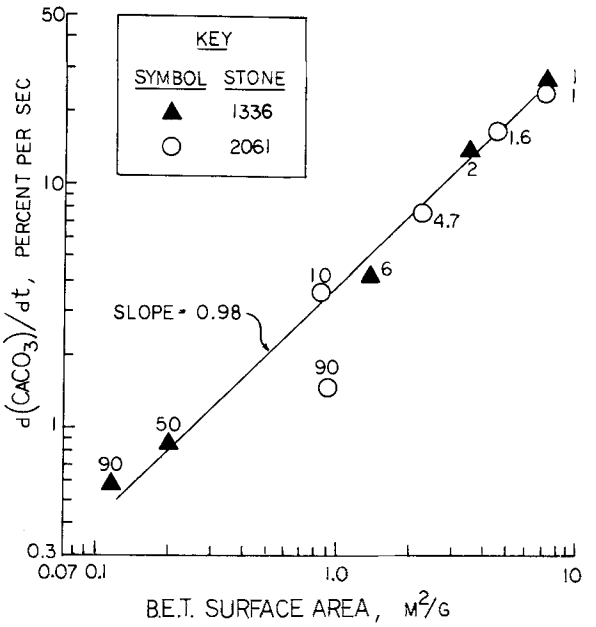

Figure 8. Calcination rate vs. initial B.E.T. surface area of limestone particles. Rates evaluated at 710°C reactor temperature, 50% conversion. Numbers by symbols denote particle diameter in μm.

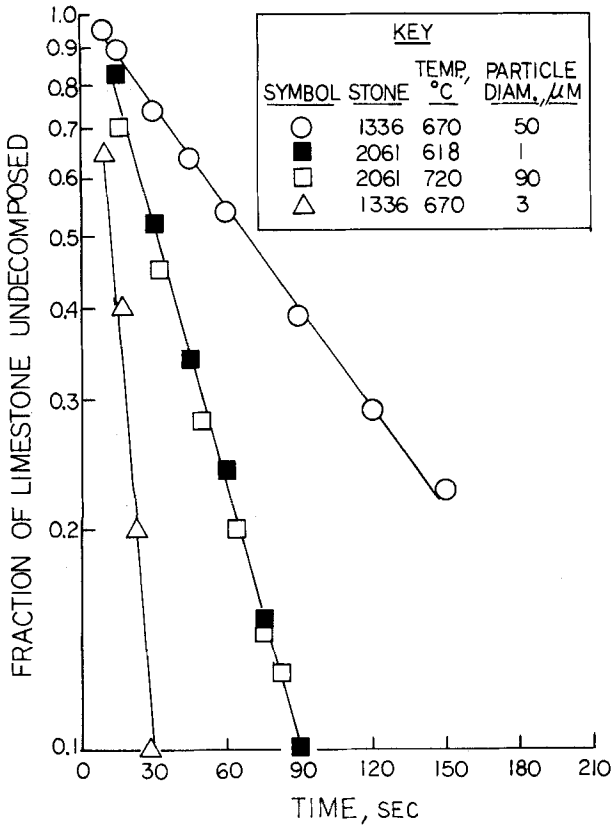

Figure 9. Test of calcination model with differential reactor data.

basis of the activation energy evaluated in Figure 7. With one exception, the calcination rate is seen to be proportional to the initial B.E.T. surface area for both stones. The exception (90 μm particles of stone 2061) can be explained by the small pore size of that stone, which is one-tenth the size of the pores in stone 1336. The slower diffusion of CO_2 through the small pores does not allow the interior of a large particle to fully participate in the calcination. When stone 2061 is reduced to 10 μm particle size, the interior pore surface becomes fully reactive and the results are in agreement with the other data. The fact that both stones correlate on the same line suggests that the calcination kinetics are intrinsic; i.e., independent of limestone type.

Assuming that the induction period of the reaction can be neglected, and (on the basis of Figure 8) that the calcination rate at time t is proportional to the B.E.T. surface area of the undecomposed $CaCO_3$, and

$$A_{CaCO_3} = S_g(CaCO_3) \tag{2}$$

the rate expression given by Eq. 1 can be integrated as:

$$\int_1^{1-x} \frac{d(CaCO_3)}{(CaCO_3)} = -k_s S_g \int_0^t dt \tag{3}$$

which yields the following calcination model for small particles:

$$\ln(1-x) = -k_s S_g t \tag{4}$$

A test of the calcination model is made in Figure 9, which shows the required linear response for both stones at various temperatures and particle sizes. Sixteen measurements of the rate constant, k_s, determined from the slopes of the lines in Figure 9 and similar plots of the other rate data, yield a mean value of 2.5×10^{-8} mol/cm^2-s with a standard deviation of ± 1.0 when normalized to a temperature of 670°C. They show no trend with stone type or particle size from 1 to 90 μm; the assumptions made in integrating the rate expression do not therefore appear to introduce serious error.

Flow Reactor

With the value of the activation energy obtained from Figure 7, the calcination model can be used to predict responses at higher

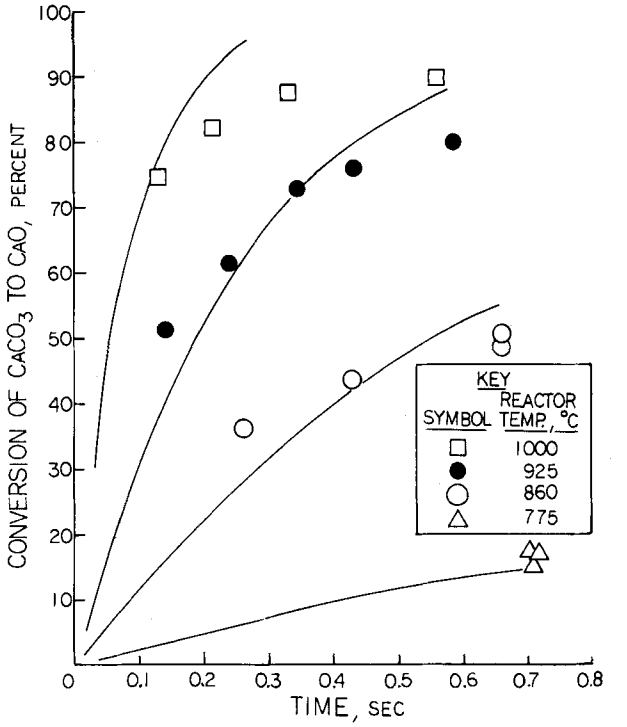

Figure 10. Predictions of kinetics model compared with experimental data from the flow reactor: 10 μm Fredonia limestone (B.E.T. surface area = 0.86 m^2/g) entrained in nitrogen.

temperatures—beyond the range of the differential reactor data. Such predictions are compared with experimental data from the entrained flow reactor in Figure 10, when injecting 10 μm particles of stone 2061 at temperatures up to 1,000°C. The data agree with the model's predictions for conversions to about 80%, indicating

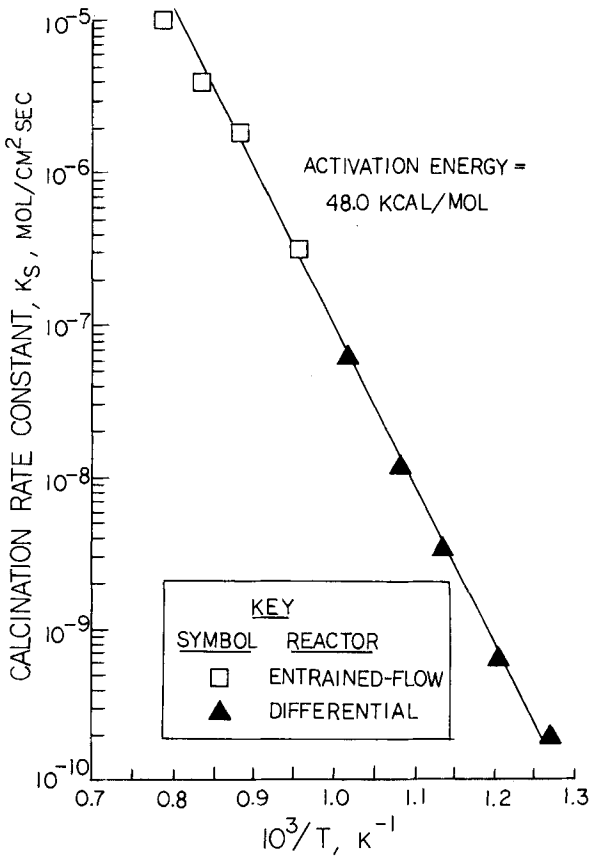

Figure 11. Comparison of rate constants derived from the flow-reactor data with rate constants derived from the differential reactor: 10 μm Fredonia limestone.

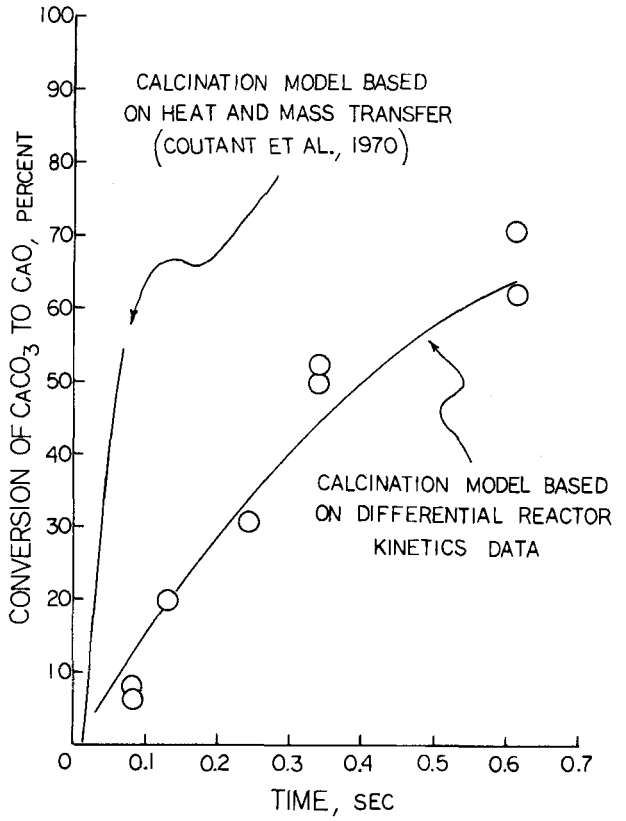

Figure 12. Calcination of 50 μm particles of Georgia marble (B.E.T. surface area = 0.20 m²/g) in the flow reactor. Comparison of experimental data with predictions of models which assume different rate-controlling mechanisms. Entrainment in nitrogen at 966°C.

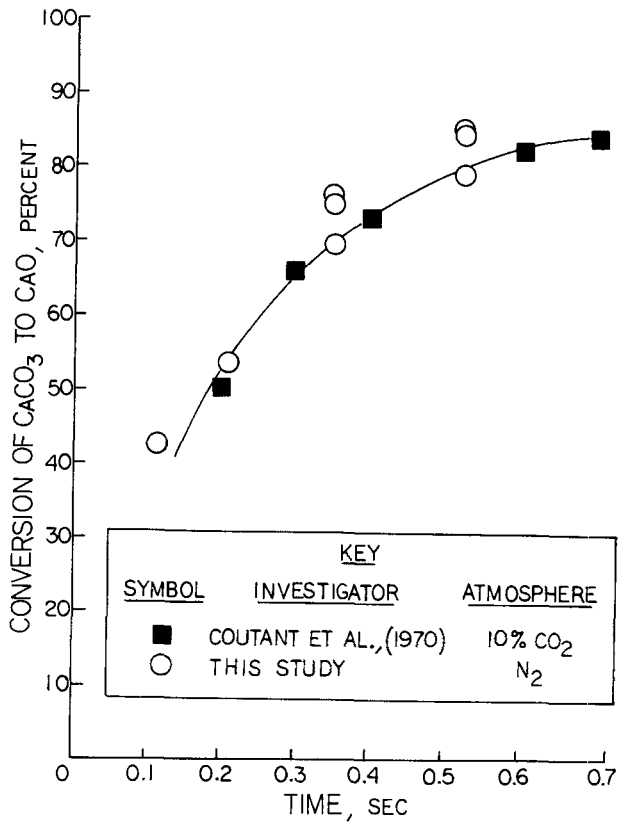

Figure 13. Comparison of calcination rates in dispersed-particle flow reactors: 90 μm limestone particles, 1,090°C.

that the calcination of 10 μm particles is dominated at these temperatures, as at lower temperatures, by chemical kinetics. Another resistance, presumably diffusion of CO_2 through the CaO, becomes significant during the final stage of decomposition.

Figure 11 compares the reaction rate constants evaluated according to Eq. 4 from the flow-reactor and differential-reactor data over the full range of temperatures studied with both systems: 516 to 1,000°C. The kinetic model correlates the data from the two reactors without discontinuity, verifying that the same mechanism controls calcination in each mode of gas/solid contacting. The activation energy indicated by the slope of the Arrhenius plot in Figure 11, fitted to both sets of data on 10 μm particles, is in good agreement with the value estimated in Figure 7 for 1 μm particles.

Comparison of the prediction of the model for a different stone and larger particle size is made in Figure 12. Again, the experimental data from the flow reactor agree with the prediction of the model for the calcination rate of 50 μm particles of stone 1336, based on its measured B.E.T. surface area. Also shown in Figure 12 is the response predicted for 50 μm particles by the Battelle heat/mass transfer model, which clearly overpredicts calcination rate.

To determine whether particle decrepitation occurred in the flow reactor, as reported by Coutant et al. (1971), samples of calcines prepared from 90 μm particles of stone 2061 and 50 μm particles of stone 1336 were resized with 200- and 325-mesh sieves, respectively. In each case, 93% of the calcine was retained by the sieve. Since the loss included the CaO abraded during sieving, it is concluded that size reduction by decrepitation was not significant at the conditions of this study.

Comparison of Results with Other Investigations

Figure 13 compares the calcination rate of 90 μm particles of stone 2061, obtained in the flow reactor, with similar data reported by Coutant et al. (1970) at the same temperature. The agreement between the two sets of data, in spite of the differences in reactor design (e.g., Coutant's reactor operated in turbulent flow), entrainment atmosphere, and sampling technique, indicates that the experimental results of this study are consistent with the existing data for limestone calcination in a dispersed system.

The activation energies estimated from this study, 48 kcal/mol (201 kJ/mol) for 10 μm particles of stone 2061 and 49 kcal/mol (205 kJ/mol) for 1 μm particles of both stones, are in good agreement with the value established by Powell and Searcy (1980) and greatly extend the valid temperature range. Their value of 49 ± 3 kcal/mol (205 ± 12.6 kJ/mol) is consistent with the results of this study over 5 orders of magnitude of reaction rate. On the basis of the measurements reported here, and the other values identified by Powell and Searcy as valid experimental determinations, a reduction in the overall error estimate to ±2 kcal/mol (±8.4 kJ/mol) is justified. The Arrhenius plots are based on the temperatures of the reactor, not the reaction interface. Satterfield and Feakes (1959)

TABLE 1. RATE CONSTANTS FOR $CaCO_3$ DECOMPOSITION AT 850°C

Investigator	Type of Measurement	Rate constant × 10^6, mol/cm²·s
Hyatt, Cutler & Wadsworth (1958)	Thin calcite crystal, nitrogen	1.0
Ingraham & Marier (1963)	6.4 mm pellets of reagent $CaCO_3$, air	1.5
Beruto & Searcy (1974)	Thin calcite crystal, vacuum	3.1[a]
Powell & Searcy (1980)	Thin calcite crystal, vacuum	1.1[a]
This paper (Figure 11)	10 μm limestone 2061, nitrogen	1.5
This paper (Figure 7)	1 μm limestone 1336, nitrogen	1.2[a]

[a] Normalized to 850°C reactor temperature on the basis of activation energy = 49 kcal/mol (205 kJ/mol).

TABLE 2. B.E.T. SURFACE AREA OF LIMESTONE PARTICLES CALCINED IN FLOW REACTOR

Reactor Temp., °C	Particle Size, μm	Residence Time, s	Calcination %	B.E.T. Surface Area, m^2/g of CaO
	Stone 2061 entrained in nitrogen, except as indicated.			
850	10	0.67	52	50
925	10	0.63	80	64
966	50[a]	0.34	52	60[a]
966	50[a]	0.61	70	55[a]
1,000	10	0.60	90	59
1,000	10	0.33	88	57
1,000	50	0.40	82	59
1,000[b]	10	0.60	94	51[b]
1,075	10	0.23	89	59
1,075	10	0.13	85	63
1,075	90	0.38	75	51

[a] Stone 1336.
[b] Entrained in air.

TABLE 3. B.E.T. SURFACE AREAS OF 1-μm LIMESTONE PARTICLES CALCINED IN DIFFERENTIAL REACTOR

	Limestone Sample Size[a]			
	100 mg		15 mg	
Reactor Temp., °C	Calcination Time, s[b]	Surface Area m^2/g	Calcination Time, s[b]	Surface Area m^2/g
600			900	90
650	1,380	49	240	88
700	450	45	90	79
750	150	40	40	76
800	70	36	15	67

[a] Multiple calcinations composited for B.E.T. analysis.
[b] 1-μm particles of stone 2061 calcined to 95 ± 5% CaO.

suggest that the absorptivity of CaO is too low to assume that these temperatures are equal and the apparent activation energy may thus include a component of radiative heat transfer. It is nevertheless clear that the calcination rate of small particles can be extrapolated on the basis of the apparent activation energy.

The other important kinentic parameter, the reaction rate constant, can be compared with several previous studies that used thin single crystals or small pellets, since the rate of CO_2 evolution should be slow enough to approach differential conditions in spite of the low sweep gas throughput. As indicated by the comparisons in Table 1, the agreement is remarkably close in most cases even though all of the other values are based on surface areas measured from the dimensions of the crystal rather than by N_2 adsorption. The six determinations listed in Table 1 yield an overall estimate of 1.6×10^{-6} mol/cm²·s at 850°C, with a standard deviation of ±0.7 mol/cm²·s.

Surface Area of CaO

Measurements of the B.E.T. surface areas of limestone particles calcined in the flow reactor at temperatures of 850 to 1,075°C are summarized in Table 2. On the basis of CaO content, the areas are consistently in the 50 to 60 m^2/g range, which confirm the highest values attained by Coutant et al. (1971). This range is also similar to the CaO surface areas found by Glasson (1958) and by Beruto et al. (1980) for vacuum calcination at low temperatures. It is thus clear that the CaO has minimum grain size [about 300 Å(30 nm) in the temperature range of these tests] and maximum surface area immediately following $CaCO_3$ decomposition. Due to rapid grain growth by sintering, the large initial CaO surface areas can be retained only at lower temperatures when using large crystals or non-differential conditions; the sintering rate increases with temperature and is independent of particle size. The fact that the large initial surface areas are retained at high temperatures when small (10 μm) particles are calcined at maximum rate implies that the calcination kinetics dominate the sintering kinetics at temperatures up to at least 1,075°C.

The data of Table 3 show that the large specific CaO surface areas obtained in the flow reactor can be reproduced by calcination in the differential reactor when the sample size is sufficiently small to ensure maximum calcination rate. In accordance with Glasson's observations (1958), the data show that the initial surface area increases as the calcination temperature is reduced; at 600°C, the corresponding CaO grain size being only 200 Å (20 nm).

To attain the greatest surface area at a given temperature, the calcination rate must be maximized. This study has shown that the maximum calcination rate is achieved when $CaCO_3$ particle size is minimized and when the decomposition occurs without mass transfer limitation; e.g. in a dispersed system.

NOTATION

A_{CaCO_3} = surface area of calcium carbonate, cm^2
$(CaCO_3)$ = undecomposed calcium carbonate in sample, mol
k_s = rate constant for surface reaction, mol/cm²·s
S_g = specific B.E.T. surface area, cm^2/mol
t = time, s
x = fractional conversion of $CaCO_3$ to CaO

LITERATURE CITED

Beruto, D., and A. W. Searcy, "Use of Langmuir Method for Kinetic Studies of Decomposition Reactions: Calcite ($CaCO_3$)," *J. Chem. Soc. Faraday Trans.*, 7, 2,145 (1974).

Beruto, D., et al., "Characterization of the Porous CaO Formed by Decomposition of $CaCO_3$ and $Ca(OH)_2$ in Vacuum," *J. Am. Ceramic Soc.*, 63, 2,972 (1980).

Borgwardt, R. H., and R. D. Harvey, "Properties of Carbonate Rocks Related to SO_2 Reactivity," *Environ. Sci. Technol.*, **6**, 350 (1972).
Caldwell, K. M., P. K. Gallagher, and D. W. Johnson, "Effect of Thermal Transport Mechanisms on the Thermal Decomposition of $CaCO_3$," *Thermochimica Acta*, **8**, 15 (1977).
Chan, R. K., K. S. Murthi, and D. Harrison, "Thermogravimetric Analysis of Ontario Limestones and Dolomites," *Canad. J. Chem.*, **48**, 2,972 (1970).
Coutant, R. W., et al., "Investigation of the Reactivity of Limestone and Dolomite for Capturing SO_2 from Flue Gas (Summary Report)," EPA Report APTD 0621 (NTIS PB 196-749), U.S. EPA, Industrial Environmental Research Laboratory, Research Triangle Park, NC (Nov. 1970).
Coutant, R. W., et al., "Investigation of the Reactivity of Limestone and Dolomite for Capturing SO_2 from Flue Gas (Final Report)," EPA Report APTD 0802 (NTIS PB 204-385), U.S. EPA, Industrial Environmental Research Laboratory, Research Triangle Park, NC (Oct. 1971).
Gallagher, P. K., and D. W. Johnson, "The Effects of Sample Size and Heating Rate on the Kinetics of the Thermal Decomposition of $CaCO_3$," *Thermochimica Acta*, **6**, 67 (1973).
Gallagher, P. K., and D. W. Johnson, "Kinetics of the Thermal Decomposition of $CaCO_3$ in CO_2 and Some Observations on the Kinetic Compensation Effect," *Thermochimica Acta*, **14**, 255 (1976).
Glasson, D. R., "Reactivity of Lime and Related Oxides," *J. Appl. Chem.*, **8**, 793 (1958).
Harvey, R. D., "Petrographic and Mineralogical Characteristics of Carbonate Rocks Related to Sulfur Dioxide Sorption in Flue Gases," EPA Report APTD 0920 (NTIS PB 206-487), U.S. EPA, Industrial Environmental Research Laboratory, Research Triangle Park, NC (July, 1971).
Hills, A. W. D., "The Mechanism of the Thermal Decomposition of Calcium Carbonate," *Chem. Eng. Sci.*, **23**, 297 (1968).
Hyatt, E. P., I. B. Cutler, and M. E. Wadsworth, "Calcium Carbonate Decomposition in Carbon Dioxide Atmosphere," *J. Am. Ceramic Soc.*, **41**, 70 (1958).
Ingraham, T. R., and P. Marier, "Kinetic Studies on the Thermal Decomposition of Calcium Carbonate," *Canad. J. of Chem. Eng.*, 170 (1963).
Powell, E. K., and A. W. Searcy, "The Rate and Activation Enthalpy of Decomposition of $CaCO_3$," *Metallurgical Trans.*, **11B**, 427 (1980).
Quann, R. J., et al., "Mineral Matter and Trace-Element Vaporization in a Laboratory-Pulverized Coal Combustion System," *Environ. Sci. Technol.*, **16**, 776 (1982).
Satterfield, C. N., and F. Feakes, "Kinetics of the Thermal Decomposition of Calcium Carbonate," *AIChE J.*, **5**, 115 (1959).

Manuscript received August 2, 1983; revision received November 23, and accepted December 5, 1983.

Reactor Selectivity Based on First-Order Closures of the Turbulent Concentration Equations

Toor's (1969) hypothesis is extended to the second-order, series-parallel reaction. A second closure relates the mixing for the second reaction to the first. The equations are solved for conversion and selectivity for a turbulent reactor configuration. The analysis is extended to incorporate concepts of residence time distribution, segregation, and maximum mixedness.

R. S. BRODKEY and JACQUES LEWALLE

Department of Chemical Engineering
The Ohio State University
Columbus, OH 43210

SCOPE

A basic understanding of turbulent motion, mixing, and kinetics in context with reactor modeling and design is not yet available to the profession. A model based on meaningful and independently measurable parameters would be helpful in reactor optimization and modification for improved performance. There have been two approaches to modeling for selectivity in chemical reactors for the second-order, series-parallel reaction. The more classic approach is to utilize single-stream residence time distribution concepts coupled with the limits of segregation and maximum mixedness and a micromixing parameter that will in some way account for the multiplicity of real effects not considered by the model, such as turbulent mixing between the inlet streams. Such models have been reviewed by Nauman (1981). The second approach, taken here, is to build a solution based on the concepts of turbulent mixing between streams, extending these concepts to the reaction in question, and utilizing them as a basis to solve the reactor performance problem. In this approach certain closure hypotheses must be made. Our goal is to further the basic understanding of reactor engineering by putting model analysis on a firmer basis.

Correspondence concerning this paper should be directed to R. S. Brodkey.
J. Lewalle is now associated with the Mechanical Engineering Department at Syracuse University, Syracuse, NY.